NANODIAMONDS IN CARBONACEOUS CHONDRITES: CONTEXTUAL CLUES OF FORMATION.
B. T. De Gregorio[1], R. M. Stroud[1], and C. M. O'D. Alexander[2], [1]U.S. Naval Research Laboratory (Code 6366, 4555 Overlook Avenue SW, Washington, DC 20375; e-mail: bradley.degregorio@nrl.navy.mil), [2]Department of Terrestrial Magnetism, Carnegie Institution of Washington.

Introduction: Nanodiamonds are present in the matrices of primitive meteorites at concentrations up to a few thousand ppm (wt. %) [1,2]. The origin of these nanodiamonds is controversial, due in part to the fact that the isotopic composition of individual ~2 nm grains cannot be reliably measured. Although Ar, Xe, Kr, and other trace element isotope signatures indicate that the nanodiamond residues contain nucleosynthetic products of supernovae, the bulk major element (C and N) isotope compositions are within solar system values. Thus, multiple formation environments are possible, including nebular, interstellar, or presolar sources [3,4]. The *in situ* petrographic context of nanodiamonds in chondrite matrices may help provide clues to their origin, if they are associated with materials of specific cosmochemical provenance. Here we extend the use of electron energy-loss spectroscopy (EELS) for locating individual nanodiamonds, established by [5], with aberration-corrected scanning-transmission electron microscopy (STEM).

Samples and Methods: Insoluble organic matter (IOM) residues were created from three primitive carbonaceous chondrites—Murchison (CM2), Elephant Moraine (EET) 92042 (CR2), and Dominion Range (DOM) 08006 (CO3)—using a multi-step HCl/CsF-HF process without boiling or centrifugation [6]. These residues contain primarily meteoritic carbonaceous matter, but also many types of acid-resistant grains [7], such as chromite and other presolar grains.

Sulfur-embedded and ultramicrotomed 90 nm thick sections were placed on lacey-carbon TEM grids and analyzed in an aberration-corrected Nion UltraSTEM 200 at 60 keV and a probe current of ~120 pA, equipped with high-angle and medium-angle annular dark field (HAADF and MAADF, respectively) detectors. This microscope includes a Gatan Enfinia EEL spectrometer and a 0.7 sr windowless Bruker energy dispersive X-ray spectrometer (EDS).

Results: Nanodiamond grains show little contrast with the surrounding carbonaceous IOM material in STEM images. Bright grains that are visible are high-Z materials, mostly chromites and other inorganic minerals (Figure 1A)[6]. However, the unique electronic band structure of diamond produces a distinct EELS spectrum to that of the surrounding IOM (Figure 1B). Using a simple metric, the change in slope between EELS spectral intensity at 285.0 eV (where C=C strongly absorbs) and 289.3 eV (at the leading edge of the diamond σ* peak), the distribution of nanodiamonds can be revealed (Figure 1C).

Alternatively, low-loss EELS and STEM-MAADF imaging can be used to efficiently locate nanodiamonds. Diamond has a bulk plasmon mode at 34 eV, whereas the IOM bulk plasmon energy lies at 23 eV (Figure 2). Since the spectral intensity in the EELS low-loss region is much higher than at the C core-loss region, nanodiamond mapping can be completed at the same level of detection in a fraction of the time.

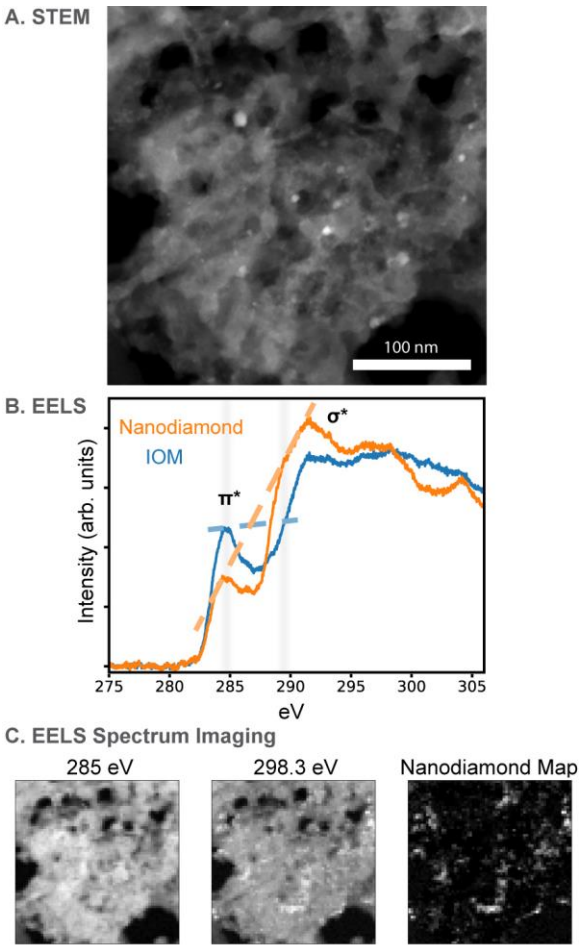

Figure 1. (A) STEM-HAADF image of Murchison IOM. Bright spots are chromites and other high-Z grains, while nanodiamonds are invisible. (B) EELS spectra of IOM and nanodiamond, showing how spectral slope can be used to distinguish the two materials. (C) EELS spectrum image slices at the energies shown in (B), along with a map of nanodiamond distribution.

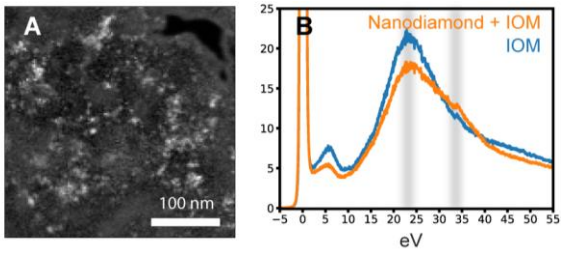

Figure 2. (A) Nanodiamond map from another area of Murchison IOM. The EELS spectrum image took ~30 seconds to acquire, in contrast to nearly 30 minutes required for the data shown in Figure 1. (B) low-loss EELS spectra showing the plasmon peak differences between IOM and diamond.

Nanodiamonds are distributed heterogenously throughout the IOM samples, found only in typical "fluffy"-textured IOM. They are absent in smooth, compact IOM and in nanoglobules (Figure 3). This may be expected, as much of the smooth and globular IOM likely formed during parent body aqueous alteration [8]. In addition, some nanodiamond clusters appear to be associated with local N enrichments of up to ~40% (Figure 4). This amount of N is too large to be wholly incorporated in the diamond grains, which average 1 at.% N, and at most compose ~10% of the sample thickness. Most of this N enrichment is associated with the enclosing IOM.

Discussion: Nanodiamonds were discovered at high abundances in each of the IOM samples. IOM-normalized abundances calculated from the nanodiamond maps by pixel counting are consistent with relative overall presolar grain abundances in these primitive chondrites (Table 1). They appear to underestimate the actual abundance by a factor of 2-3x, although this could be compensated by the ~50% yield from the IOM extraction.

Our preliminary data indicate that nanodiamond clusters may be associated with N-rich IOM. This suggests that the formation process of these clusters would also be associated with the production of N-rich organic matter. Isotopic measurements are necessary to constrain possible formation environments. Supernovae are typically ^{15}N poor, while ^{15}N enrichments could indicate a molecular cloud or outer nebula origin. An inner nebular origin, such as incomplete conversion of N-rich organics during nebular shocks, would maintain a solar ^{15}N composition.

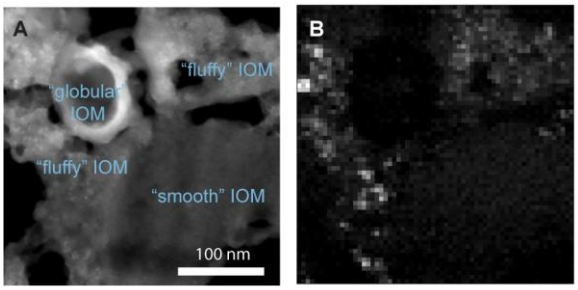

Figure 3. (A) STEM-HAADF image of Murchison IOM showing several common textures, including a nanoglobule. (B) Nanodiamond map, revealing that diamond grains are only present in "fluffy" IOM.

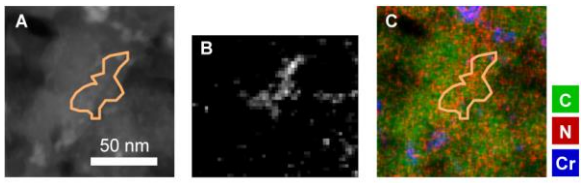

Figure 4. (A) STEM-MAADF image of an invisible cluster of nanodiamonds in Murchison IOM. (B) Corresponding diamond map. (C) Corresponding EDS map indicating a ~40% enrichment in N.

Future work will involve characterization of IOM-bearing matrix samples extracted by FIB-SEM methods. It is expected that nanodiamonds located in these FIB sections will be isolated enough to obtain isotopic measurements from small clusters or possibly even single nanodiamond grains.

Acknowledgements: The authors thank L. R. Nittler for helpful conversation regarding calculating nanodiamond grain abundances.

References: [1] Lewis R. S. et al. (1987) *Nature* 328, 160-162. [2] Huss, G. R. et al. (2003) *GCA* 67, 4823-4848. [3] Dai Z. R. et al. (2002) *Nature* 418, 157-159. [4] Stroud R. M. et al. (2011) *ApJ Lett.* 738, L27. [5] Garvie L. A. J. (2010) *LPSC XLI*, abstract #1388. [6] Alexander C. M. O'D. et al. (2018) *GCA* 221, 406-420. [7] Chizmadia L. et al. (2018) presented at 2018 AGU, Washington, DC, abstract P52B-05. [8] Cody G. D. et al. (2011) *PNAS* 108, 19171-19176. [9] Koch I. and Floss C. (2017) *LPSC XLVIII*, abstract #2984. [10] Nittler L. R. et al. (2018) *GCA* 226, 107-131.

Table 1. Nanodiamond Abundance in Chondrites

Sample	Murchison	EET 92042	DOM 08006
Type	CM2	CR2	CO3
Nanodiamond Abundance (ppm)			
Literature	1164 [2]	-	-
IOM Normalized	18005	4246	14188
Matrix Normalized	571	164	855
SiC Abundance (ppm)	14 [2]	10 [9]	35 [10]